Journal of Photochemistry and Photobiology A: Chemistry 200 (2008) 307–313

Contents lists available at ScienceDirect

Journal of Photochemistry and Photobiology A: Chemistry

journal homepage: www.elsevier.com/locate/jphotochem

Photophysical behavior of lipophilic xanthene dyes without the involvement of photoinduced electron transfer mechanism

Xian-Fu Zhang[a,*], Qiang Liu[b], Hanbin Wang[a], Zheng Fu[a], Fiishi Zhang[b]

[a] Chemistry Department, Hebei Normal University of Science and Technology, Qinghuangdao, Hebei Province 066004, China
[b] Chemistry Department, Tsinghua University, Beijing 100084, China

ARTICLE INFO

Article history:
Received 30 January 2008
Received in revised form 10 July 2008
Accepted 16 August 2008
Available online 27 August 2008

Keywords:
Xanthene dye
Fluorescein
Fluorescence
Aggregation
Lipase

ABSTRACT

The correlation of dibutyl-ether-ester of xanthene dye structures with their photophysical properties is discussed with respect to their capability as fluorescent probes based on ultraviolet–visible absorption, fluorescence spectra and fluorescence lifetimes measured in different solvents. It was found that the dibutyl-ether-ester of fluorescein is very weakly emissive in aprotic solvents, but fairly strong fluorescent in alcohols. The dependence of fluorescence quantum yield (Φ_f) and lifetime (τ_f) on solvent polarity suggests non-involvement of the intra-molecular photoinduced electron transfer (PeT) mechanism, suggested previously to account for the emission efficiency of fluorescein derivatives. The xanthene dyes intend to self-assemble in aprotic solvents, less polar solvents facilitate the aggregation while hydrogen bonding disfavor it. The formation of non-emissive H-aggregates is proposed to be responsible for their fluorescent behavior. The esterification showed stronger influences on the photophysics than the etherification, i.e. the former caused larger reduction of Φ_f owing to the internal conversion. The halogenation decreases the fluorescence quantum yield and lifetime of the xanthene dyes, owing to the enhancement of inter-system crossing process.

1. Introduction

Lipophilic fluorescein derivatives (dibutyl-ether-ester in Scheme 1) have been employed to detect lipases since 1960s [1–5], because the enzyme activity is strongly related to the dyes fluorescence intensity. The lower polarity of such compounds than their parent compounds ($R_1 = R_2 = H$ in Scheme 1) makes them easier to enter into, bind and react with intra-cellular enzymes. The other advantage is their ability to avoid the coexistence of the prototropic and lactone forms that often make the system complicated and less efficient for fluorescein and eosin [6,7].

While the photophysics of the dianions ($R_1 = R_2 = Na$ in Scheme 1) has been the focus of many studies [8–17], little attention is paid to the neutral form of xanthene dyes. This is mainly because the quinoid cannot be isolated but always coexists with at least one of the three species, i.e. monoanion, lactone or dianion attributed to acid dissociation and tautomerization as shown in Scheme 1 [18]. So is the case for the monoanion. The monoester and dialkyl-ether-ester are both good models for the quinoid. The latter, however, is easier to prepare by using excessive halogenoalkane and no laborious separation needed.

The mechanism that controls the fluorescence efficiency of xanthene dyes has also been a focus for the rational design of fluorescent probes, the lipophilic fluorescein derivatives also serve as the models to understand the mechanism [19–27]. Photoinduced electron transfer (PeT), for example, has been suggested to account for the emissive behavior of fluorescein derivatives and design new probes meeting different needs [19–27]. Other possible mechanisms have not been explored, however.

With these considerations in mind, herein we report the synthesis and photophysics of dibutyl-ether-ester of xanthene dyes, which should be helpful for the better understanding and interpretation of spectra of such fluorescence probes. It is found that these dyes can strongly self-assemble into H-type non-emissive aggregates and the heavy halogeno-atoms showed profound effect on the photophysical properties. Furthermore the dependence of Φ_f and τ_f on solvent polarity shows that the PeT mechanism is not an important factor to control the emission efficiency of the xanthene dyes.

2. Experimental part

2.1. Materials

The dianion sodium of xanthene dyes (dye content >90%) and reagent grade 1-bromo-*n*-butane were purchased from Beijing

* Corresponding author. Fax: +86 10 627 70304.
E-mail address: zhangxianfu@tsinghua.org.cn (X.-F. Zhang).

1010-6030/$ – see front matter © 2008 Elsevier B.V. All rights reserved.
doi:10.1016/j.jphotochem.2008.08.008

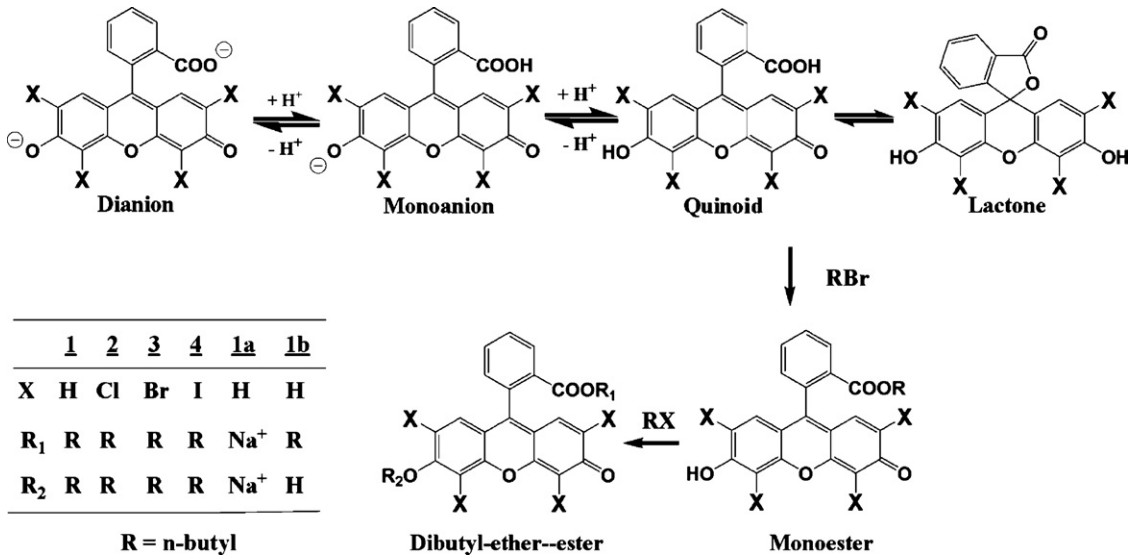

	1	2	3	4	1a	1b
X	H	Cl	Br	I	H	H
R_1	R	R	R	R	Na^+	R
R_2	R	R	R	R	Na^+	H

Scheme 1.

Chemical Company and purified according to the procedure by Markuszewski and Diehl [28]. The other solvents are all analytical grade and redistilled before measuring spectra.

2.2. Apparatus and spectrum measurements

Ultraviolet–visible (UV–vis) absorption spectra were recorded using a Shimadzu UV-240 Spectrophotometer or HP 8452A with a matched pair of quartz cuvettes. Fluorescence spectra were taken in a PE LS-50 Spectrofluorimeter with a slit width of 2.5 nm and excitation at 410 nm, duplicate spectral measurements were taken at a constant temperature, 22 °C, and the mean values were used for data analysis. Fluorescence quantum yields were calculated by using fluorescein (in 0.1 M NaOH aqueous solution) as reference ($\Phi_f = 0.91$). Doubly distilled water was used for solution preparation. For all fluorescence measurements, the corresponding blank sample solutions were checked first and found no significant signals. Fluorescence lifetime measurements were made with Edinburgh FL920 time-correlated single photon counting spectrophotometer with excitation at 430 nm and emission at 550 nm.

2.3. Synthesis

2.3.1. General procedure for the synthesis of di-ether-ester

To a 15 ml of DMF containing 0.01 mol dianion sodium of xanthene dye, 0.03 mol 1-bromo-*n*-butane and 0.06 mol potassium carbonate were added. After 6 h stirring and heating at 85 °C, 100 ml cold water was added. The resulting precipitate was filtered, washed with deionized water thoroughly and dried.

2.3.2. Butyl 2-(6-butoxy-3-oxo-3H-xanthen-9-yl) benzoate (1)

The product was purified by column chromatography using hexane as mobile phase. Yield 73%. ^{1}H NMR (δ, $CDCl_3$): 0.75 (3H, t), 0.95 (3H, t), 1–2 (8H, m), 3.93 (2H, t), 4.10 (2H, t), 6.50–6.70 (2H, m), 6.80 (1H, d), 6.85–7.10 (3H, m), 7.30 (1H, d), 7.70–7.80 (2H,t) and 8.25 (1H, d). MS (M^+): 444. IR (cm^{-1}) (KBr): 3052, 1714, 1637 and 1592.

2.3.3. Butyl 2-(6-hydroxy-3-oxo-3H-xanthen-9-yl)benzoate (1b)

The molar ratio of xanthene to *n*-butyl bromide was changed to 1:0.95. The product was purified by column chromatography using ethyl acetate as mobile phase. Yield 53%. ^{1}H NMR (δ, ^{d}DMSO): 0.66 (3H, t), 0.95–1.19 (4H, m), 3.89 (2H,t), 6.28 (2H, s), 6.32 (2H, d), 6.61 (2H, d), 7.42 (1H, d), 7.72 (1H, t), 7.80 (1H, t) and 8.12 (1H, d). MS (M^+): 388. IR (cm^{-1}) (KBr): 3421, 3058, 1720, 1636 and 1578.

Butyl 2-(6-butoxy-2,4,5,7-tetrachloro-3-oxo-3*H*-xanthen-9-yl) benzoate (**2**). The product was purified by column chromatography using hexane–acetone (20:1) as mobile phase. Yield 67%. MS: 582.02 (M+H), ^{1}H NMR ($CDCl_3$) δ: 6.86–7.00 (d, 2H), 6.70–6.85 (s, 2H), 6.48 (d, 1H), 6.31 (s, 1H), 4.06 (t, 2H), 3.93 (t, 2H), 1.00–1.90 (m, 8H), 0.90–1.00 (t, 3H) and 0.62–0.75 (t, 3H).

2.3.4. Butyl 2-(6-butoxy-2, 4, 5, 7-tetrabromo-3-oxo-3H-xanthen-9-yl) benzoate (3)

The product was purified by column chromatography using dichloromethane as mobile phase. Yield 59%. MS: 759.9 (M+H), ^{1}H NMR ($CDCl_3$) δ: 8.26 (t, 1H), 7.60–7.80 (m, 2H), 7.16 (d, 1H), 6.96 (d, 1H), 6.82 (d, 1H), 4.14 (t, 2H), 4.00 (m, 2H), 1.00-2.00 (m, 8H), 0.95 (m, 3H) and 0.78 (m, 3H).

2.3.5. Butyl 2-(6-butoxy-2, 4, 5, 7-tetraiodo-3-oxo-3H-xanthen-9-yl) benzoate (4)

The product was purified by column chromatography using dichloromethane as mobile phase. Yield 15.5%. MS: 747.9 (M+H), ^{1}H NMR ($CDCl_3$) δ: 8.00 (d, 1H), 7.60–7.80 (m, 2H), 7.15 (m, 1H), 6.73 (d, 1H), 6.59 (d, 1H), 3.90–4.20 (m, 4H), 1.00–2.10 (m, 8H), 0.85–1.00 (m, 6H).

3. Results and discussion

3.1. Synthesis

Commercially available xanthene dyes are in either their disodium salt or lactone forms. Both can be used as starting materials for the synthesis in the presence of potassium carbonate and excessive 1-bromo-*n*-butane in acetone or DMF. The carboxyl group is more reactive and mono-esterified xanthenes are the major products if the molar ratio of starting materials is not more than 1:1. The dianion is preferred since the lactones can also yield the byproducts containing dietherified lactones. In the case of the tetra-iodinated xanthene dye, however, the mono-esterified product was obtained as the major product even in the presence of large excessive 1-bromo-*n*-butane, which is likely caused by the steric hindrance of two adjacent iodine atoms of the hydroxyl group.

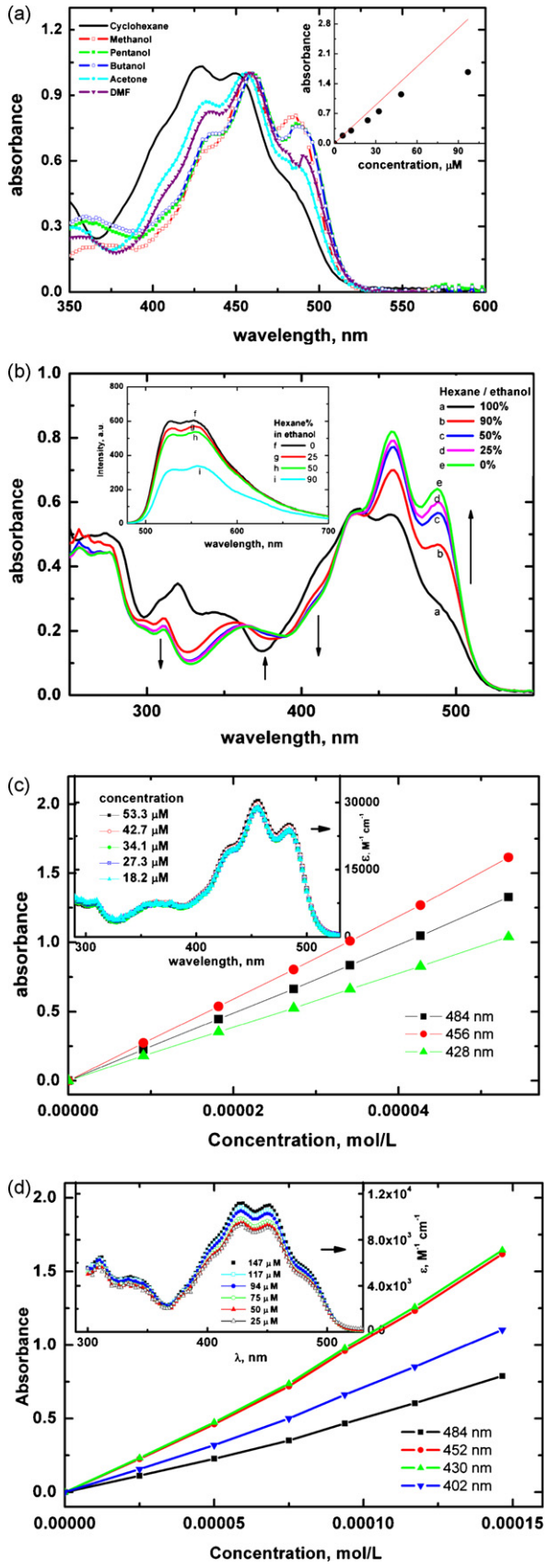

Fig. 1. (a) The absorption spectra of 1 (ca. 40 μM) in different solvents. Inset: a plot of absorbance against concentration in acetone at 458 nm. (b) The absorption spectra of 1 (30 μM) in ethanol–hexane mixtures. Inset: the effect of hexane on the fluorescence spectra of 1 (λ_{ex}: 410 nm), the spectrum in neat hexane is not shown because its fluorescence quantum yield is nearby zero. (c) The absorption maxima and spectra (inset, molar absorption coefficient at different λ) of 1 in methanol as a function of concentration. (d) The absorption maxima and spectra (inset, molar absorption coefficient at different λ) of 1 in hexane as a function of concentration. (For interpretation of the references to color in the artwork, the reader is referred to the web version of the article.)

3.2. Absorption spectra and self-aggregation

During the measurements it was found that solvents and dye concentration showed strong influences on the absorption and fluorescence spectra of **1**. Comparing any two UV–vis spectra of Fig. 1a in different solvents, the decline in the red band of the right most (band III) is always concomitant with the rise of the blue band around 435 nm (band I). The Beer law is deviated significantly with the increase of the dye concentration as shown in the inset of Fig. 1a (such as that in acetone) except for that in methanol (Fig. 1c).

In ethanol–hexane binary solvent, by increasing the volume ratio of hexane while keeping the concentration of compound **1** constant, the spectra in Fig. 1b showed rough isosbestic points at 362, 388 and 432 nm. Once again, the going up of the blue band is accompanied by the dropping down of the red band. The presence of the isosbestic points indicates the equilibrium between the monomer of **1** and the aggregate. The corresponding fluorescence spectra, however, showed almost identical shape although the intensity is decreased remarkably with the increase of the molar ratio of hexane (inset of Fig. 1b). This suggests that no new emission band occurs, and the formed aggregate is non- or very weakly emissive.

This observation matches the H-type aggregation behavior of aromatic dyes [30–32], i.e. dyes are self-associated through face-to-face approaching. The extent of deviation from Beer's law in alcohols is much less obvious than that in aprotic solvents, such as hexane, suggests that the inter-molecular association in the alcohol is much less efficient. The spectra of compound **1** as a function of its concentration in methanol and hexane are shown in Fig. 1c and d, respectively. In methanol, a linear relation is found when the dye concentration is less than 53 μM, indicating negligible aggregation. While in hexane, the deviation from Beer's law is obvious. Compound **1** is almost completely aggregated in hexane even when the concentration of **1** is as low as 25 μM, which is suggested by (i) a hundred times decrease in the fluorescence quantum yield in hexane as compared with methanol; (ii) a much lower molar absorption coefficient (about one-third of that in methanol) and distinct absorption spectra in hexane. The higher aggregates may form with the increase of concentration of **1** in hexane, which explains the deviation from both Beer's law and isosbestic point in Fig. 1b.

According to the relative height of the peaks in a spectrum, the spectra can be grouped roughly in two types: protic and aprotic solvents. In protic solvents, the height ratio of band III over band I (>1.05) is remarkably larger than that in aprotic solvents (<0.76). The typical examples are methanol and hexane, respectively. In each group of solvents, with the decrease of solvent polarity the relative absorption intensity of band I is enhanced, while that of band III is weakened. This indicates that lower polarity favors the aggregation in each group of two types of solvents, respectively. But the aggregation in protic solvents is much less important than that in aprotic solvents.

The fluorescence quantum yield (Φ_f, Table 1) in alcohols is much higher than that in aprotic solvents because of much weaker aggregation. This is consistent with the known fact that H-aggregates are non-fluorescent [29–32]. The reduction of the aggregation by alcohols is owing to its capability of forming hydrogen bond between an

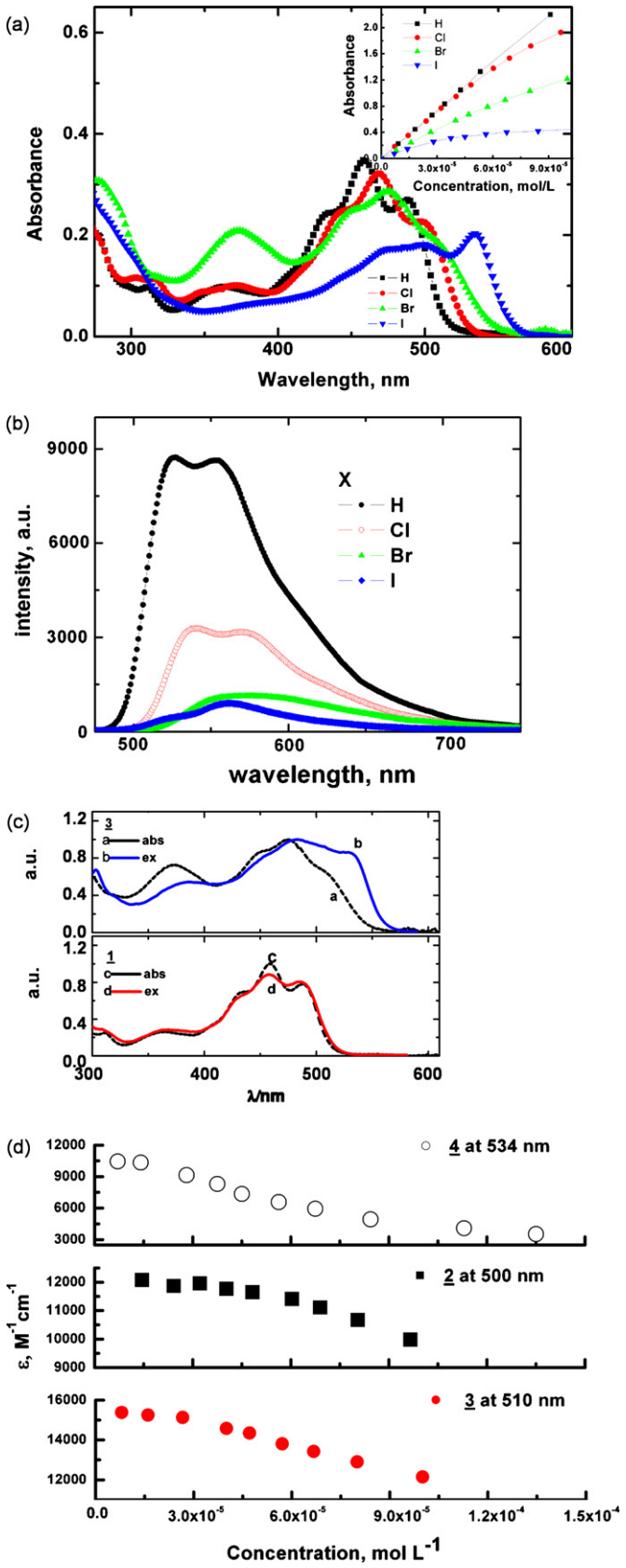

Fig. 2. (a) Absorption spectra of 1–4 in methanol (concentration is adjusted between 10 and 15 μM). Inset is the plots of absorption maxima against dye concentrations. (b) Fluorescence spectra of 1–4 in methanol, λ_{ex} = 410 nm, absorbance at excitation wavelength was adjusted to be 0.10. (c) The comparison of excitation spectrum with corresponding absorption spectrum. (d) Plot of molar absorption coefficient as a function of total concentration. (For interpretation of the references to color in the artwork, the reader is referred to the web version of the article.)

Table 1
Fluorescence quantum yield and lifetime in different solvents

	Φ_f				τ_f (ns)
	1	**2**	**3**	**4**	**1**
DMF	0.056	–	–	–	–
Methanol	0.35	0.12	0.060	0.021	2.8
Acetone	0.034	–	–	–	–
n-Butanol	0.27	0.095	0.046	0.014	2.7
n-Pentanol	0.28	–	–	–	–
Chloroform	0.15	–	–	–	–
Toluene	0.0038	–	–	–	–
n-Hexane	0.0035	0.0012	0.015	0.009	2.1
Cyclohexane	0.00073	–	–	–	–

alcohol's hydroxyl and the ether or carbonyl oxygen of compound **1**.

Comparing the fluorescence lifetime of **1** in methanol, butanol and hexane, it shows no increase but a slight decrease in the latter two less polar solvents. The fluorescence quantum yield, on the other hand, is dramatically lowered by more than one hundred times. This is another evidence to support the formation of non-emissive H-type aggregates.

This H-type aggregation also occurs in compounds **2**–**4** as shown in Fig. 2, but the aggregation tendency follows **1** < **2** < **3** < **4** as judged by (i) comparing the ratio of band III over band I in Fig. 2 and (ii) the degree of deviation from Beer's law shown in the inset of Fig. 2a. In Fig. 2c, the excitation spectra were compared with the corresponding absorption spectra. In the case of **1**, the difference between the two spectra is slight which also indicates a negligible aggregation. For the other three compounds such as **3** in Fig. 2c, it is found that the decrease of red band in absorption spectra is accompanied by the increase of blue band owing to the aggregation behavior.

Assuming a dimerization equilibrium between monomer M and dimer D:

$$2M \leftrightarrows D, \text{ with equilibrium constant } \mathbf{K},$$

we could evaluate the equilibrium constant lg **K** to be 3.3, 3.7 and 4.9 for dyes **2**–**4**, respectively from the data in inset of Fig. 2a.

What is particular interesting is that the dependence of τ_f of **1** on solvent polarity is contradictive to the PeT mechanism, in which the higher the polarity the shorter the τ_f is expected. The PeT mechanism has been suggested by Miura et al. to account for the emission efficiency of fluorescein derivatives and to design new fluorescent probes [19–21]. In this model, the benzene moiety and xanthene ring in a dye are considered to be the electron donor (or acceptor) and electron acceptor (or donor) responsible for PeT. Clearly in the system of this study, however, PeT does not play important roles for **1**.

It is, therefore, concluded that the di-ether-ester compounds intend to self-assemble into H-type non-emissive aggregates. Low polarity favors the assembly while hydrogen bonding can hinder their formation. In the following discussion of photophysics, the spectra were therefore measured in methanol with sufficient low dye concentration to minimize the aggregation.

3.3. *Effect of alkylation on the photophysics*

The alkylation can be performed on either hydroxyl at position 6 or carboxyl group at position 1′ of the dyes, as shown in Scheme 2, but the latter is easier to carry out.

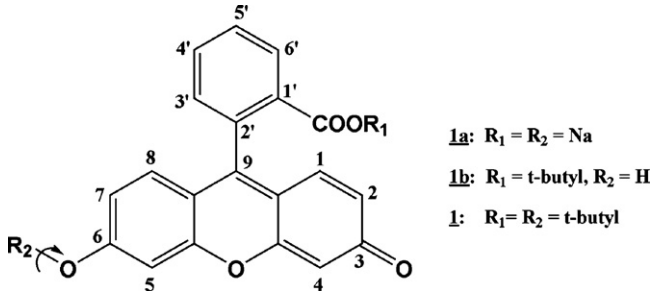

Scheme 2.

Both alkylations showed remarkable effect on the fluorescence properties. Fig. 3 compares the UV–vis absorption characteristics of three compounds **1a**, **1b** and **1** and their corresponding fluorescence emission spectra. Similar to **1**, both **1a** and **1b** did not show aggregation in methanol. The dibutyl-ether-ester **1** shows similar peak patterns to that of monoester **1b** in the visible region, but with a slight blue shift and a change of relative peak height. The disodium salt of fluorescein **1a**, in contrast, shows more red shifted, sharper but simpler peaks. The π system of **1a** contains one more electron (the negative charge) than compound **1**, therefore the two compounds have different HOMOs and also different energy gaps between HOMO and LUMO. This explains the very different spectra of **1a** from **1**.

The fluorescence spectra in Fig. 3 indicate that **1** has the longest emission maximum although it has the shortest abs. maximum, which means that it has the largest stokes shift of 89 nm compared to 44 nm for **1b**, and 40 nm for **1a**.

Three compounds **1a**, **1b** and **1** showed very different fluorescence quantum yields in methanol, decreased remarkably in the order from 0.92 (**1a**) to 0.50 (**1b**) and 0.35 (**1**). From the value of Φ_f (0.92) for **1a** and its chemical structure in Scheme 2, we know that the internal conversion caused by the rotation of benzene moiety contributes less than 8% to the total decay rate constant of S_1 of **1a**. In **1b** and **1**, the contribution is expected to be even less because of the more bulky esterified benzene moiety. This reveals that the covalent bonding of hydrogen or butyl to the oxygen at position 6 (see Scheme 2) is responsible for the decrease of Φ_f in **1b** and **1** compared to that of **1**, i.e. the rotation along the O–R_2 (see Scheme 2) promotes the internal conversion from the lowest excited singlet

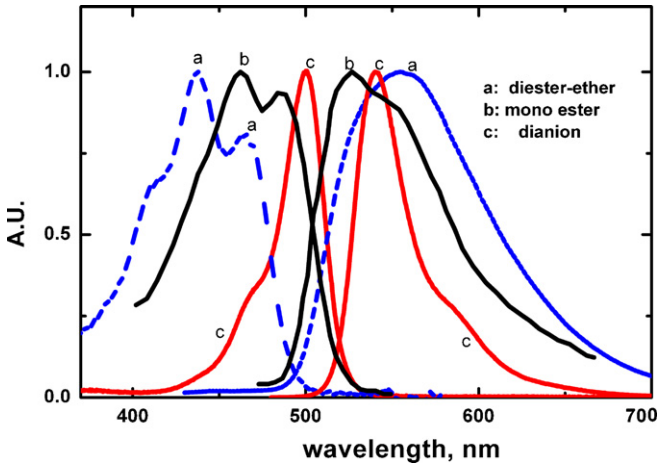

Fig. 3. Normalized absorption and emission spectra of 1, 1a and 1b in methanol. λ_{ex} = 410 nm, absorbance at excitation wavelength was adjusted to be 0.10. (For interpretation of the references to color in the artwork, the reader is referred to the web version of the article.)

Table 2
Effect of alkylation on photophysical parameters in methanol

	λ_{abs}^{max} (nm)	λ_{em}^{max} (nm)	E_s (eV)	Φ_f	τ_f (ns)	k_f ($\times 10^9$ s^{-1})	k_{nr} ($\times 10^9$ s^{-1})
1a	500	540	2.39	0.92	4.2	0.22	0.019
1b	484	527	2.46	0.50	5.3	0.094	0.094
1	466	555	2.51	0.35	2.8	0.13	0.24

state to the ground state. The butyl group exerted a more profound effect than the hydrogen atom.

The change in fluorescence lifetime (τ_f) for **1b** and **1** compared to that of **1a** is not so significant as that of Φ_f. The value of τ_f is 4.2 ns for dianion **1a**, 5.3 ns for **1b** and 2.8 ns for **1**, respectively. Since $\tau_f = (k_f + k_{nr})^{-1}$ and $\Phi_f = k_f\tau_f$, in which k_f and k_{nr} are the radiative and non-radiative decay rate constant respectively, we then obtain the values of k_f ($=\Phi_f/\tau_f$) and k_{nr} [$=(1-\Phi_f)/\tau_f$] as collected in Table 2. E_s is the energy for the lowest lying excited singlet state.

Comparing the k_f and k_{nr} value in Table 2, we can see that the enhancement of non-radiation decay by alkylation is remarkable, it is more significant than the decrease of radiation constant from **1a** to **1**. Comparing **1b** to **1** in which the only difference of structures is an H atom is replaced by a butyl, we can see that the alkyl bonding to oxygen at position 6 causes a stronger internal conversion of the excited state of fluorescein.

3.4. Influences of halogenations on the photophysical properties

Electron transfer mechanism has been proposed to tune the emission efficiency of fluorescent probes, heavy atom effect, however, is another alternative. It enhances usually the triplet quantum yield while decreases the fluorescent efficiency. Furthermore, the presence of heavy atoms is known to promote the decay via phosphorescence. Strong phosphorescence or delayed fluorescence is often desirable for some applications, such as OLED. We therefore consider to evaluating the heavy atom effect on the emission efficiency and lifetime of lipophilic xanthenes.

The absorption spectra are compared in Fig. 2a. Two major effects can be observed, i.e. the red shift of absorption maximum and the relative rise of the band at 372 nm. The former is related to the electron donating ability in the order of H < Cl < Br < I, while the latter is likely caused by the promoted p–π conjugation. Fig. 2b shows the emission spectra, the emission maximum is red shifted in the same order as that observed in the absorption spectra. As mentioned before (ξ3.2), from Fig. 2a **2**–**4** show the aggregation behavior with the tendency **1** < **2** < **3** < **4**.

The fluorescence quantum yield (after correcting the influence of aggregation by using the calculated dimerization constants), however, was declined remarkably, from 0.35 for **1** to 0.061 for **4**. This mainly reflects the enhanced inter-system crossing (ISC) from S_1 to T_1 state.

The fluorescence decay traces are shown in Fig. 4a. They are well fitted by monoexponential decay, which once again confirmed that the aggregates are non-emissive. The emission lifetimes become shorter with the increase of the size of the substituted halogeno atoms. The extent of decrease, however, is almost as large as that of emission efficiency. This means that k_f, the emission rate constant, is kept constant according to $k_f = \Phi_f/\tau_f$. These values are listed in Table 3.

Similar to the dianion salt of halogenated xanthene dyes, for which the sum of the quantum yields of fluorescence and triplet state formation is equal to unity within experimental error [15], the rate constants of internal conversion for **1**–**4** are not expected to change significantly, i.e. the change of emission caused by halogenation is almost solely caused by the enhancement of inter-

Table 3
Photophysical parameters in methanol[a]

	λ_{abs}^{max} (nm)	λ_{em}^{max} (nm)	E_S (eV)	Φ_f	τ_f (ns)	k_f ($\times 10^9$ s^{-1})	Δk_{isc} ($\times 10^9$ s^{-1})
1	458, 486	526	2.44	0.35	2.80	0.125	0
2	468, 496	540	2.38	0.15	1.35	0.110	0.384
3	476, 514	553	2.30	0.081	0.61	0.130	1.28
4	500, 534	561	2.27	0.061	0.52	0.117	1.57

[a] Fluorescence quantum yield is corrected to the value for monomers by the method in ref. [29].

system crossing. The change of k_{isc} is therefore calculated by

$$\Delta k_{isc} = \frac{1}{\tau_f} - \frac{1}{\tau_f^0}, \quad (1)$$

where τ_f and $1/\tau_f^0$ refer to the observed excited singlet state lifetime in the presence and absence of halogenations.

According to a classical theory [33], k_{isc} may be expressed in the following form:

$$k_{isc} = B(C^* C_x \zeta)^2, \quad (2)$$

where B refers to the rate constant for ISC in the absence of heavy atom substituents (k_{isc} for **1** in this case). For substitution at fixed sites, C^* and C_x can be taken as constants. ζ is the atomic spin-orbit coupling constant for halogen atoms (587, 2460 and 5060 for Cl, Br, and I respectively). We have then

$$lg(k_{isc}) = \text{constant} + lg(\zeta)^2. \quad (3)$$

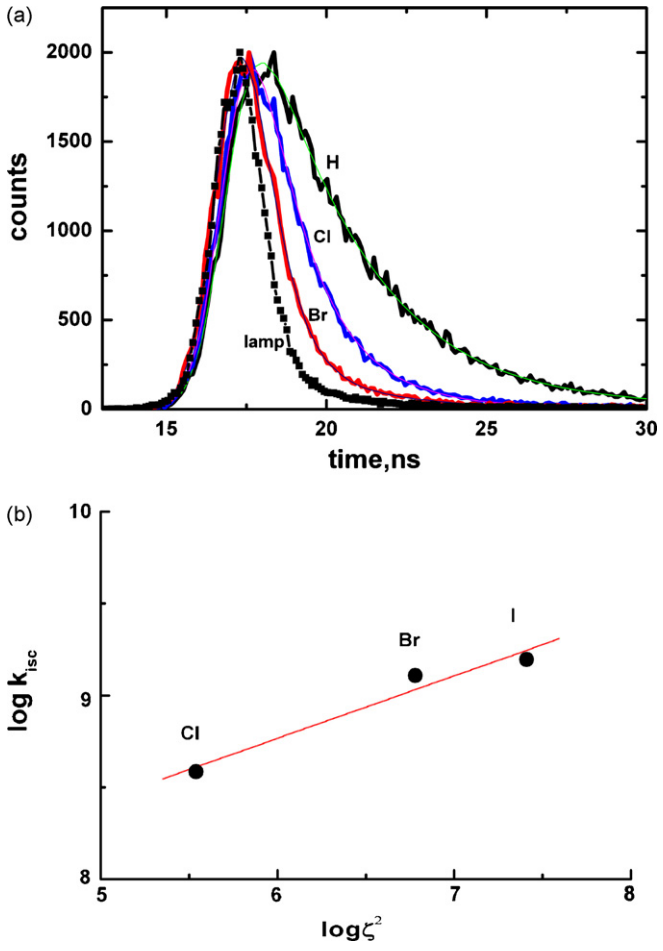

Fig. 4. (a) Fluorescence decay of 1–3 in methanol, λ_{ex} = 430 nm, λ_{em} = 550 nm, absorbance at excitation wavelength was adjusted to be 0.15. (b) Halogenation effect treated by Eq. (3). (For interpretation of the references to color in the artwork, the reader is referred to the web version of the article.)

Fig. 4b shows the plot of $\lg(\Delta k_{isc})$ against $\lg(\zeta)^2$. A linear correlation indicates that the observed change in photophysical properties is indeed due to the promotion of ISC.

This work has remarkable implications on the using lipophilic fluorescein derivatives as fluorescence probes to detect lipases. It is shown here that the fluorescence intensity of the probes is strongly affected by the hydrogen bonding capability and polarity of the surrounding medium, owing to the aggregation behavior. This means that the strong enhancement of fluorescence intensity may not always be caused by catalyzed hydrolysis of probes by the lipases but by the change of micro-media surrounding probes. To overcome this effect, the non-aggregated probes should be designed and prepared.

4. Conclusion

The di-ether-ester of xanthene dyes **1**–**4** intend to self-assemble in aprotic solvents, weak polarity facilitates the aggregation while hydrogen bonding disfavor it. The formation of non-emissive H-type aggregates is responsible for their fluorescence behavior. PeT, on the other hand, is not likely to play important roles for **1**. The esterification showed stronger influences on the photophysics than the etherification, i.e. the former caused larger reduction of Φ_f owing to the internal conversion. The halogenations decrease the Φ_f and τ_f, which can be attributed to the enhancement of intersystem crossing.

Acknowledgement

We thank the Key Laboratory of Photochemistry, Chinese Academy of Sciences for financial support.

References

[1] D.N. Kramer, G.G. Guilbault, Anal. Chem. 35 (1963) 588–589.
[2] G.G. Guilbault, D.N. Kramer, Anal. Chem. 36 (1964) 409–412.
[3] G.G. Guilbault, M.H. Sadar, Anal. Lett. 1 (1968) 551–553.
[4] G.G. Guilbault, J. Hieserman, J. Am. Chem. 41 (1969) 2006–2009.
[5] J.R. Falck, M. Krieger, J.L. Goldstein, M.S. Brown, J. Am. Chem. Soc. 103 (1981) 7396–7398.
[6] H. Diehl, N. Horchak-Morris, Talanta 34 (1987) 739–741.
[7] H. Diehl, Talanta 36 (1989) 413–415.
[8] L.N. Domelsmith, L.L. Munchausen, K.N. Houk, J. Am. Chem. Soc. 99 (1977) 4306–4311.
[9] P. Bilski, R. Dabestani, C.F. Chignell, J. Phys. Chem. 95 (1991) 5784–5791.
[10] L. Flamigni, J. Phys. Chem. 97 (1993) 9566–9572.
[11] S. Reindl, A. Penzkofer, Chem. Phys. 213 (1996) 429–438.
[12] S.K. Lam, D. Lo, Chem. Phys. Lett. 281 (1997) 35–43.
[13] S.K. Lam, E. Namdas, D. Lo, J. Photochem. Photobiol. A: Chem. 118 (1998) 25–30.
[14] S. Biswas, S.C. Bhattacharya, P.K. Sen, S.P. Moulik, J. Photochem. Photobiol. A: Chem. 123 (1999) 121–128.
[15] H. Gratz, A. Penzkofer, J. Photochem. Photobiol. A: Chem. 127 (1999) 21–30.
[16] D. Magde, G.E. Rojas, P.G. Seybold, Photochem. Photobiol. 70 (1999) 737–744.
[17] D. Magde, R. Wong, P.G. Seybold, Photochem. Photobiol. 75 (2002) 327–334.
[18] V. Zanker, Chem. Ber. 91 (1958) 572–575.

[19] T. Miura, Y. Urano, K. Tanaka, T. Nagano, K. Ohkubo, S. Fukuzumi, J. Am. Chem. Soc. 125 (2003) 8666–8671.
[20] T. Ueno, Y. Urano, K.-I. Setsukinai, H. Takakusa, H. Kojima, K. Kikuchi, K. Ohkubo, S. Fukuzumi, T. Nagano, J. Am. Chem. Soc. 126 (2004) 14079–14085.
[21] Y. Urano, M. Kamiya, K. Kanda, T. Ueno, K. Hirose, T. Nagano, J. Am. Chem. Soc. 127 (2005) 4888–4894.
[22] J. He, J. Zhao, T. Shen, H. Hidaka, N. Serpone, J. Phy. Chem. B 101 (1997) 9027–9034.
[23] B. Jing, M. Zhang, T. Shen, Org. Lett. 5 (2003) 3709–3711.
[24] H. Zhang, Y. Zhou, M. Zhang, T. Shen, Y. Li, D. Zhu, J. Phys. Chem. B 106 (2002) 9597–9603.
[25] B.A. Sparano, K. Koide, J. Am. Chem. Soc. 129 (2007) 4785–4794.
[26] S. Yoon, E.W. Miller, Q. He, P.H. Do, C.J. Chang, Angew. Chem. Int. Ed. 46 (2007) 6658–6661.
[27] S. Yoon, A.E. Albers, A.P. Wong, C.J. Chang, J. Am. Chem. Soc. 127 (2005) 16030–16031.
[28] R. Markuszewski, H. Diehl, Talanta 27 (1980) 937–946.
[29] X.-F. Zhang, H. Xu, J. Chem. Soc., Faraday Trans. 89 (1993) 3347–3351.
[30] E. Rabinowitch, L. Epstein, J. Am. Chem. Soc. 63 (1941) 69–75.
[31] W. West, S. Pearce, J. Phys. Chem. 69 (1965) 1894–1903.
[32] U. Roesch, S. Yao, R. Wortmann, F. Wuerthner, Angew. Chem. Int. Ed. 45 (2006) 7026–7030.
[33] S.P. McGlynn, T. Azumi, M. Kinoshita, Molecular Spectroscopy of the Triplet State, Prentice Hall, Englewood Cliffs, NJ, 1969.